Title

A joint estimation detection of Glaucoma progression in 3D spectral domain optical coherence tomography optic nerve head images

Authors

Belghith, Akram

Bowd, Christopher

Weinreb, Robert N

et al.

Publication Date

2014-03-18

DOI

10.1117/12.2041980

Peer reviewed

Published in final edited form as:
Proc SPIE. 2014 March 18; 9035: 90350O–. doi:10.1117/12.2041980.

A joint estimation detection of Glaucoma progression in 3D spectral domain optical coherence tomography optic nerve head images

Akram Belghith, **Christopher Bowd**, **Robert N. Weinreb**, and **Linda M. Zangwill**
Hamilton Glaucoma Center, University of California San Diego, La Jolla, California

Abstract

Glaucoma is an ocular disease characterized by distinctive changes in the optic nerve head (ONH) and visual field. Glaucoma can strike without symptoms and causes blindness if it remains without treatment. Therefore, early disease detection is important so that treatment can be initiated and blindness prevented. In this context, important advances in technology for non-invasive imaging of the eye have been made providing quantitative tools to measure structural changes in ONH topography, an essential element for glaucoma detection and monitoring. 3D spectral domain optical coherence tomography (SD-OCT), an optical imaging technique, has been commonly used to discriminate glaucomatous from healthy subjects. In this paper, we present a new framework for detection of glaucoma progression using 3D SD-OCT images. In contrast to previous works that the retinal nerve fiber layer (RNFL) thickness measurement provided by commercially available spectral-domain optical coherence tomograph, we consider the whole 3D volume for change detection. To integrate a priori knowledge and in particular the spatial voxel dependency in the change detection map, we propose the use of the Markov Random Field to handle a such dependency. To accommodate the presence of false positive detection, the estimated change detection map is then used to classify a 3D SDOCT image into the “non-progressing” and “progressing” glaucoma classes, based on a fuzzy logic classifier. We compared the diagnostic performance of the proposed framework to existing methods of progression detection.

Keywords

Glaucoma; Markov field; change detection; fuzzy logic classifier

1. INTRODUCTION

Glaucoma is an optic neuropathy in which the eye’s internal pressure increases and causes nerve fiber damage in the optic nerve. The increase in intraocular pressure (IOP) is generally due to either a malformation or a malfunction of the eye’s drainage system.[1]

Initially asymptomatic for several years, the glaucoma develops gradually and painlessly. Untreated, elevated IOP causes loss of peripheral vision and, in an advanced state,

Further author information: (Send correspondence to A. Belghith), A. Belghith: abelghith@ucsd.edu, Telephone: (+1) (858) 822-1465.

irreversible blindness. However, early detection and treatment can slow, or even halt the progression of the disease. Hence, it is important to develop clinical routines for progression detection in order to avoid permanent damage to the optic nerve head.

Since Hermann von Helmholtz invented the ophthalmoscope in 1851, physicians were able to visualize damages in the optic nerve head associated with glaucoma. However, clinical examination of the ONH remains subjective, qualitative and variably reproducible.[2]

Over the past two decades, innovations in computer-based ocular imaging technologies using the optical properties of the optic nerve and retinal nerve fiber RNFL layer have gained widespread use in the diagnosis and management of glaucoma patients. Specifically, the advent of optical coherence tomography (OCT) provided a noninvasive optical imaging technique that has been used to evaluate structural changes in the ONH and RNFL layer in vivo. Recently, spectral domain OCT (SD OCT) advances have brought a significant improvement in image capture speed and resolution and exhibit some of the characteristics of a good diagnostic tool such as high sensitivity and specificity, good reproducibility, ability to detect change over time, simplicity in usage and interpretation and convenience for both patient and physician.[3]

In this context, automatic image processing methods are regularly proposed to assist the expert in the qualitative and quantitative analysis. These methods aim to facilitate the interpretation of the obtained images by objectively measuring the ONH structure and detecting changes between a reference image (a baseline exam) and other images (follow-up exams).

A numerous studies have been published on glaucoma detection using SD-OCT images. Most of the studies use the RNFL measurements to discriminate glaucomatous from healthy subjects.[4–6] RNFL thickness measurements are assigned to categorical classes such as ‘glaucomatous’, ‘borderline’, or ‘normal’ classes based on a comparison with a normative database. This classification allows clinicians to assess the structural status of glaucoma objectively and conveniently. However, although this method has been successfully applied to SD-OCT images, its use is constrained by a specific pre-requisite: it requires an accurate estimation of the RNFL layer thickness. However, authors of[7] showed that poor quality images affects the accuracy of the RNFL layer thickness estimation. Moreover, the RNFL-feature based methods do not exploit additional constraints often available, such as voxel spatial dependency (*i.e*, the status of a voxel will depend on the status of its neighborhood) and noise characteristics. We show in this paper that glaucoma detection can be more robust, more accurate and more efficient if such information is integrated and correctly modeled within the change detection method.

In this paper, we propose a new strategy for glaucoma progression detection using the 3D SD-OCT images. This strategy is divided into two steps:

1. Change detection: it consists of detecting changes between a baseline image and a follow-up image and a classification step which consists in classifying the detected changes into random changes or true changes due to glaucoma progression. For the first task, we propose a fully Bayesian framework for change detection. Bayesian

methods are relatively simple and offer efficient tools to include *priori* through *a posteriori* probability density function PDF. In particular, we propose the use of the Markov Random Field (MRF) to exploit the statistical correlation of intensities among the neighborhood voxels.[8] In order to develop a noise robust algorithm, we propose consideration of the change detection problem as a missing data problem where we jointly estimate the noise hyperparameters and the change detection map. The most widely used procedure to estimate the different problem parameters is the Expectation-Maximization EM algorithm.[9] However, since we used the MRF model with the change detection map as the prior for the change detection map, the optimization step is intractable. Hence, we propose the use of a Monte Carlo Markov Chain (MCMC) technique.[10]

2. Classification: once the change detection map is estimated, we propose the use of a new fuzzy classifier which aims at classifying a SD-OCT image into the "non-progressing" and the "progressing" glaucoma classes based on the estimated change detection map. What adds difficulty to automating this process is that stable or normal non-progressing SD-OCT images may present with some detectable changes. The primary causes of non-progressing eye changes are image registration errors and variation in the diameter of retinal vessel.[11] To overcome this drawback, a threshold-based classification method may be used to accommodate the presence of false positive detection.[12] However, the choice of the threshold (usually 5% of the number of voxels) may affect the robustness of the classification method. If we decrease the threshold value, the risk of false negative classifications increases and similarly if we increase the threshold value, the risk of having false positive classifications will increase. To circumvent this problem, we will use the fuzzy set theory which is well suited to model such ambiguity. Specifically, the importance of fuzzy set theory stems from the fact that much of the information on which human decisions are based, in our case glaucoma progression detection, is possibilistic rather then deterministic.[13]

The paper is divided into two sections. In section 2, the proposed glaucoma change detection scheme is presented. We describe in section 3 the classification scheme. Then, in section 4 results obtained by applying the proposed scheme to real data are presented. We then compare the diagnostic accuracy, robustness and efficiency of this novel proposed approach compared to two existing progression detection RNFL based approaches: the Artificial Neural Network classifier (ANN) and the Support vectors Machine classifier.[14]

2. CHANGE DETECTION

2.1 Direct model

Let us consider the detection of changes in a pair of amplitude images. We denote by I_0 and I_1 two images acquired over the same eye at times t_0 and t_1, respectively ($t_1 > t_0$), and coregistered. In this work, we assume that the noise is additive, white and normally distributed. In addition, the gamma distribution is used to model the *a priori* knowledge we have on the free noise SD-OCT images. Indeed, the gamma distribution has been successfully used to fit spectral data that may present a background.[15] The direct model for

both images I_0 and I_1 is then given by: $I_0 = X_0 + N_0$ and $I_1 = X_1 + N_1$ where $X_0 \sim \mathcal{G}(\alpha_0, \beta_0)$ and $X_1 \sim \mathcal{G}(\alpha_1, \beta_1)$ are the noise free 3D SD-OCT ONH images:

$$p(x_0,\alpha_0,\beta_0)=\frac{x_0^{\alpha_0-1}}{\Gamma(\alpha)\beta^{\alpha_0}}\exp\left(-\frac{x_0}{\beta}\right),\ p(x_1,\alpha_1,\beta_1)=\frac{x_1^{\alpha_1-1}}{\Gamma(\alpha)\beta^{\alpha_1}}\exp\left(-\frac{x_1}{\beta}\right)\quad x_0,x_1>0 \quad (1)$$

and $N_0 \sim \mathcal{N}(0, \sigma_0)$ and $N_1 \sim \mathcal{N}(0, \sigma_1)$ are additive, white and normally distributed noises. Change-detection can be formulated as a binary hypothesis testing problem where the null hypothesis of "H_0: No change" is tested against the alternative hypothesis of "H_1: Change"

In this work, we consider the following direct model: $R=\frac{I_0}{I_1}=\frac{X_0+N_0}{X_1+N_1}$. However, this model is intractable. To overcome this problem, we propose a hierarchical change detection framework which consists of estimating the noise free SD-OCT images $\hat{X_0}$ and $\hat{X_1}$ and then use the image ratio approach for change detection. The direct model is then given by $R=\frac{\hat{X}_0}{\hat{X}_1}$. The gamma ratio distribution is expressed as:

$$p(r(i);\alpha_0,\beta_0,\alpha_1,\beta_1)=\frac{\Gamma(\alpha_0+\alpha_1)}{\Gamma(\alpha_0)\Gamma(\alpha_1)}r(i)^{\alpha_0-1}\left(\frac{\beta_0}{\beta_1}\right)^{\alpha_0}\left(r(i)+\frac{\beta_0}{\beta_1}\right)^{-(\alpha_0+\alpha_1)} \quad (2)$$

In case where $\alpha_0 = \alpha_1 = \alpha$ and $\beta=\frac{\beta_0}{\beta_1}$, $p(r(i); \alpha, \beta)$ is given by;

$$p(r(i);\alpha,\beta)=\frac{\Gamma(2\alpha)}{\Gamma(\alpha)^2}r(i)^{\alpha-1}\beta^{\alpha}(r(i)+\beta)^{-2\alpha} \quad (3)$$

Finally, the change detection is handled through the introduction of change class assignments Q. To introduce a spatial *a priori* knowledge on ($Q = (q_i)_{i=1:M}$), we used the Markov model so that the change status $q(i)$ of a voxel $r(i)$ depends on the change status of its neighborhood.

2.2 The estimation scheme

The Bayesian model aims at estimating the model parameters (X_0, X_1, Q) and hyperparameters Θ. This requires defining of the likelihood and prior distributions. We now present each term of the hierarchical Bayesian model.

Likelihood—The definition of the likelihood depends on the noise model. As we assumed that the noise in both images I_0 and I_1 is white and normally distributed with standard deviations σ_0 and σ_1 respectively, the likelihood is then given by:

$$p(I_0|X_0;\sigma_0)=\mathcal{N}(0,\sigma_0);\quad p(I_1|X_1;\sigma_1)=\mathcal{N}(0,\sigma_1) \quad (4)$$

Model prior—The prior on X_0 and X_1 is given by the gamma density $\mathcal{G}$:

$$p(X_0;\alpha_0,\beta_0)=\prod_{i=1}^{M}\mathcal{G}(x_0(i),\alpha_0,\beta_0);\quad p(X_1;\alpha_1,\beta_1)=\prod_{i=1}^{M}\mathcal{G}(x_1(i),\alpha_1,\beta_1) \quad (5)$$

To describe the marginal distribution of R conditioned to $H_{l,l\in\{1,2,3\}}$, we used the ratio gamma distribution:

$$p(R|Q=H_l;\theta_l,\kappa_l)=\prod_{i=1:M}\frac{\Gamma(2\theta_l)}{\Gamma(\theta_l)^2}r(i)^{\theta_l-1}\kappa_l^{\theta_l}(r(i)+\kappa_l)^{-2\theta_l} \quad (6)$$

Concerning the change variable, we assume that $p(Q;\Theta)$ is a spatial Markov prior. In this study we adopt the Potts model with interaction parameter ζ:

$$p(Q;\zeta)=\frac{1}{Z}\exp(-\zeta U(Q)),\quad U(Q)=\sum_{i\sim j}\delta(q_i,q_j) \quad (7)$$

where Z is the normalization constant and δ the delta Kroneker function. Note that we have opted for the 6-connexity 3D neighboring system. By combining the likelihood and the prior knowledge using the Bayes' rule and giving our hierarchical approach we adopted, the obtained posterior distribution $p(Q, \Theta|R)$ is intractable for our model. Hence, we propose the use of a Monte Carlo Markov Chain (MCMC) procedure to estimate the model parameters and hyperparameters. As in,[16] we use a Gibbs sampler based on a stationary ergodic Markov chain allowing to draw samples whose distribution asymptotically follows the *a posteriori* densities.

3. CLASSIFICATION

Once the change detection maps are estimated, we now tackle the glaucoma progressor image classification problem. This step aims at assigning an image to the non-progressor or the progressor classes. To this end, a two-layer fuzzy classifier is proposed. In contrast to,[12] no threshold is required. In our case, the fuzzy set theory is used to quantify the membership degrees of a given image to each class (*i.e*; progressor and non-progressor). It's important to note that the fuzzy classifier we propose can be trained using only the control data (non-progressor eyes) as in some cases, no prior knowledge of the changes due to glaucoma progression is available.

As in,[12] we considered two features as input for the classifier: 1) *feature*1: the number of changed sites and 2) *feature*2: the residual image intensity R of changed sites. Note that only the loss of retinal height in neighboring areas is considered change due to glaucomatous progression because an increase in retinal height is considered improvement (possibly due to treatment or tissue rearrangement).

We now calculate the elementary membership degree to the non-progressor class given each feature $\gamma_{nor,o\in\{feature1,feature2\}}$ using a S-membership function f whose expression is given in Eq. 8. Note that the range $[a, c]$ defines the fuzzy region.

$$f(x;a,b,c)=\begin{cases}0 & x<a\\ \frac{(x-a)^2}{(b-a)\,(c-a)} & a\le x<b\\ 1-\frac{(x-c)^2}{(c-b)\,(c-a)} & b\le x<c\\ 1 & \text{otherwise}\end{cases} \quad (8)$$

where $a < b < c$.

$$\gamma_{nor}=\gamma_{nor,feature1}\times\gamma_{nor,feature2} \quad (9)$$

where $\gamma_{nor,feature1} = f(N_c; a_1, b_1, c_1)$, $\gamma_{nor,feature2} = f(\Sigma_{i\in C} R_i; a_2, b_2, c_2)$, N_c and C stand for the number of changed sites and the changed site class respectively and (a_1, b_1, c_1, a_2, b_2, c_2) are the hyperparameters of the S-membership functions. The hyperparameters (a_1, b_1, c_1, a_2, b_2, c_2) are estimated with the Genetic algorithms[17] using longitudinal SD-OCT data from a training dataset which contains 10 normal eyes, 5 non-progressing eyes and 10 progressing eyes. Note that the training dataset is independent of the test dataset described in section 4. The membership degree to the glaucoma class γ_{glau} is given by:

$$\gamma_{glau}=1-\gamma_{nor} \quad (10)$$

To decide if a given SD-OCT image belongs to the glaucoma progressor class, another membership function is used. We opted for the trapezoidal function denoted by g as a membership function. The expression of g is given by:

$$g(x;a_3,b_3,c_3,d_3)=\begin{cases}\left(\frac{x-a_3}{b_3-a_3}\right) & a_3\le x<b_3\\ 1 & b_3\le x<c_3\\ \left(\frac{d_3-x}{d_3-c_3}\right) & c_3\le x<d_3\\ 0 & \text{otherwise}\end{cases} \quad (11)$$

where $a_3 < b_3 < c_3 < d_3$. Alternately, the Genetic algorithm was used to estimate this quadruple. The decision to classify an image into the glaucoma class depends on the output of the function $g(\gamma_{glau})$. As can be observed, g function depends on the quadruple (a_3, b_3, c_3, d_3) as well as on (a_2, b_2, c_2) and (a_1, b_1, c_1). If $g(\gamma_{glau}) = 1$ the image is assigned to the glaucoma progressor class.

4. RESULTS

This section describes the glaucoma progression detection results obtained with the proposed scheme. A summary of the method is presented in Fig. 1.

In order to perform the classification evaluation, we have retained the *sensitivity* and the *specificity* measurements:

$$sensitivity=\frac{TP}{TP+FN};\quad specificity=\frac{TN}{TN+FP}$$

where *TP* stands for the number of true positive identifications, *FN* the number of false negative identifications and *FP* the number of false positive identifications.

The proposed framework was experimentally validated with real datasets. Diagnostic accuracy was estimated using 117 eyes of 75 participants. Sensitivity was estimated in 27 eyes classified as progressing by standardized assessment of stereophotographs by 2 independent graders and/or by designation as 'likely progression' based on visual field Guided Progression Analysis (Humphrey Visual Fields, Carl Zeiss Meditec, Dublin, CA) (mean follow-up 4 years, 4 tests). Specificity was estimated using 50 stable glaucoma eyes (imaged once a week for 5 consecutive weeks) and using 40 healthy eyes (mean follow-up 3 years, 3 tests). It is important to note that we used independent training and test sets to estimate the diagnostic accuracy of the methods. In order to emphasize the benefit of the proposed glaucoma progression detection scheme, we have compared the proposed framework called as **Fuzzy Baysian detection scheme (FBDS)** to:

1. The SVM classifier of the RNFL thickness. As in,[14] we used the radial basis function as kernel. The SVM was trained by a variation of Platt's sequential minimal optimization algorithm.[18] The SVM hyperparameters were determined by a global optimization technique based on simulated annealing[19] (RNFL-SVM).
2. The ANN classifier of the RNFL thickness. As in,[14] we used the Multiayer perceptrons version of the ANN[20] (RNFL-ANN).
3. The proposed method without the MRF *a priori* on the change detection map (FDS).
4. The proposed method with a threshold classifier (T-DS).

Results are presented in Tab. 1. The FBDS method with the use of the whole 3D SD-OCT volume instead of the RNFL measurements results in high specificity in both normal and stable glaucoma eyes (94% and 92% respectively) while maintaining good sensitivity (64%) in the progressing eyes. Moreover, one can see that the use of the MRF *a priori* and the fuzzy classifier increases both specificity and sensitivity.

5. CONCLUSION

In this paper, a new framework for glaucoma progression detection has been proposed. We particularly focus on the formulation of the change problem as a missing data problem. The task of inferring the glaucomatous changes is tackled with a hierarchical MCMC algorithm that is used for the first time to our knowledge in the glaucoma diagnosis framework. The validation of the proposed approach with real data has shown better diagnosis accuracy for glaucoma detection compared to existing methods.

Acknowledgments

The authors acknowledge the funding and support of the National Eye Institute (grant numbers: U10EY14267, EY019869, EY021818, EY022039 and EY08208, EY11008, P30EY022589 and EY13959).

References

1. Dielemans I, De Jong PT, Stolk R, Vingerling JR, Grobbee DE, Hofman A, et al. Primary open-angle glaucoma, intraocular pressure, and diabetes mellitus in the general elderly population. the rotterdam study. Ophthalmology. 1996; 103(8):1271. [PubMed: 8764798]
2. Jaffe GJ, Caprioli J. Optical coherence tomography to detect and manage retinal disease and glaucoma. American journal of ophthalmology. 2004; 137(1):156–169. [PubMed: 14700659]
3. Chen TC, Cense B, Pierce MC, Nassif N, Park BH, Yun SH, White BR, Bouma BE, Tearney GJ, de Boer JF. Spectral domain optical coherence tomography: ultra-high speed, ultra-high resolution ophthalmic imaging. Archives of Ophthalmology. 2005; 123(12):1715. [PubMed: 16344444]
4. Vizzeri G, Balasubramanian M, Bowd C, Weinreb RN, Medeiros FA, Zangwill LM. Spectral domain-optical coherence tomography to detect localized retinal nerve fiber layer defects in glaucomatous eyes. Optics express. 2009; 17(5):4004. [PubMed: 19259242]
5. Sung KR, Kim DY, Park SB, Kook MS. Comparison of retinal nerve fiber layer thickness measured by cirrus hd and stratus optical coherence tomography. Ophthalmology. 2009; 116(7):1264–1270. [PubMed: 19427696]
6. Chang, Robert T.; Knight, O.; Feuer, WJ.; Budenz, DL. Sensitivity and specificity of time-domain versus spectral-domain optical coherence tomography in diagnosing early to moderate glaucoma. Ophthalmology. 2009; 116(12):2294–2299. [PubMed: 19800694]
7. Balasubramanian M, Bowd C, Vizzeri G, Weinreb RN, Zangwill LM. Effect of image quality on tissue thickness measurements obtained with spectral-domain optical coherence tomography. Optics express. 2009; 17(5):4019. [PubMed: 19259243]
8. Li, SZ. Markov random field modeling in computer vision. Springer-Verlag; New York, Inc: 1995.
9. McLachlan, GJ.; Krishnan, T. The EM algorithm and extensions. Vol. 274. Wiley; New York: 1997.
10. Gilks, WR.; Richardson, S.; Spiegelhalter, DJ. Markov chain Monte Carlo in practice. Chapman & Hall/CRC; 1996.
11. Harris A, Ciulla TA, Chung HS, Martin B. Regulation of retinal and optic nerve blood flow. Archives of ophthalmology. 1998; 116(11):1491. [PubMed: 9823351]
12. Balasubramanian M, Kriegman DJ, Bowd C, Holst M, Weinreb RN, Sample PA, Zangwill LM. Localized glaucomatous change detection within the proper orthogonal decomposition framework. Investigative Ophthalmology & Visual Science. 2012; 53(7):3615–3628. [PubMed: 22491406]
13. Waltz, E.; Llinas, J., et al. Multisensor data fusion. Vol. 685. Artech House; Norwood, MA: 1990.
14. Bizios D, Heijl A, Leth Hougaard J, Bengtsson B. Machine learning classifiers for glaucoma diagnosis based on classification of retinal nerve fibre layer thickness parameters measured by stratus oct. Acta ophthalmologica. 2010; 88(1):44–52. [PubMed: 20064122]
15. Belghith A, Collet C, Armspach JP. Change detection based on a support vector data description that treats dependency. Pattern Recognition Letters. 2012
16. Belghith, A.; Collet, C.; Armspach, JP. Computational Surgery and Dual Training. Springer; 2014. A statistical framework for biomarker analysis and hr-mas 2d metabolite identification; p. 89-112.
17. Goldberg, DE. Genetic Algorithms in Search and Optimization. Addison-wesley; 1989.
18. Fan RE, Chen PH, Lin CJ. Working set selection using second order information for training support vector machines. The Journal of Machine Learning Research. 2005; 6:1889–1918.
19. Imbault, F.; Lebart, K. A stochastic optimization approach for parameter tuning of support vector machines. Pattern Recognition, 2004. ICPR 2004. Proceedings of the 17th International Conference on IEEE; 2004; p. 597-600.
20. Gardner MW, Dorling SR. Artificial neural networks (the multilayer perceptron)–a review of applications in the atmospheric sciences. Atmospheric environment. 1998; 32(14–15):2627–2636.

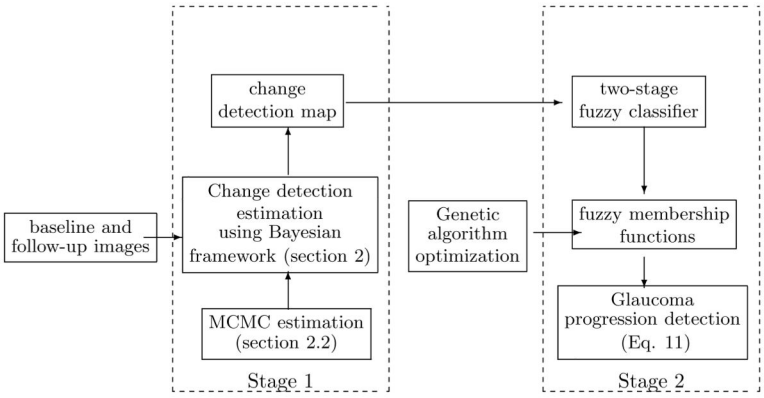

Figure 1.
Overview diagram of glaucoma progression detection scheme

Table 1

Diagnostic Accuracy of different methods.

	Progressor group sensitivity	Normal group specificity	Stable group specificity
FBDS	**64** %	**92** %	**94** %
FDS	55 %	82 %	85 %
T-DS	58 %	85 %	87 %
RNFL-ANN	49 %	71 %	78 %
RNFL-SVM	52 %	68 %	79 %